Journal of Alloys and Compounds 505 (2010) 443–449

Contents lists available at ScienceDirect

Journal of Alloys and Compounds

journal homepage: www.elsevier.com/locate/jallcom

Conditions for preparation of nanosized $Al_2(WO_4)_3$

V. Nikolov, I. Koseva*, R. Stoyanova, E. Zhecheva

Institute of General and Inorganic Chemistry, Bulgarian Academy of Sciences, Acad. G. Bonchev Str., Building 11, 1113 Sofia, Bulgaria

ARTICLE INFO

Article history:
Received 31 March 2010
Received in revised form 8 June 2010
Accepted 13 June 2010
Available online 25 June 2010

Keywords:
Nanostructured materials
Tungstates
Chemical synthesis
X-ray diffraction
Transmission electron microscopy
Thermal analysis

ABSTRACT

Pure nanosized $Al_2(WO_4)_3$ was synthesized according to different methods—solid state synthesis with and without preliminary mechanical activation, co-precipitation and sol–gel method. Structure and morphology of $Al_2(WO_4)_3$ were determined by powder XRD diffraction and TEM analysis. It was found that the co-precipitation method gives lowest in size, uniform particles (22 nm), distributed in very narrow size region (10–40 nm), expanding more than four times during the thermal treatment. This product seems to be suitable as a starting material for $Al_2(WO_4)_3$ transparent ceramics.

1. Introduction

Aluminium tungstate is a representative of the class of the $Me_2(WO_4)_3$ compounds, where Me = Y, Sc, In, Al, as well as the rare earth elements from Ho to Lu with orthorhombic structure of the $Sc_2(WO_4)_3$ type (space group *Pnca*) [1]. This class of compounds possesses Al^{3+} ion conductivity [2–4] unusual low even negative thermal expansion coefficient [5–7]. $Me_2(WO_4)_3$ compounds doped by Cr^{3+} are very perspective laser media for tunable lasers [8].

However, the production of single crystals as laser active media from these tungstates is related with a number of problems, first of all due to significant evaporation of WO_3 in the case of Czochralski growth [9–12] or low growth velocity and anisotropy [13–15].

An effective approach to overcoming the crystal growth problems is to produce transparent ceramics, replacing the single crystals. A number of research works on Nd:$Y_3Al_5O_{12}$ ceramics show that in this way it is possible to obtain optical materials with desired size and homogeneous composition and properties [16–19].

The technology of optical ceramics includes three main stages: fabrication of nanopowders; preparing of highly dense compacts and sintering of the compact to the non-porous ceramics [20]. Many investigations show, that to fabricate transparent ceramics ultrafine, monosized low-agglomerated nanopowders with high sintering activity have to be preliminary obtained [21–25].

In this communication we report data on the synthesis of nanosized $Al_2(WO_4)_3$ by three methods: classical solid state reaction, solid state reaction after mechanical activation, sol–gel and precipitation methods. A special attention was paid on the effect of the synthesis procedure the powder size, shape, size distribution and sintering activity of the obtained powders.

2. Conditions for synthesis and methods for characterization

Three different methods were applied for producing $Al_2(WO_4)_3$—solid state synthesis, co-precipitation and sol–gel (modified method of Pechini). Each of these methods was tested under different conditions as described below.

2.1. Solid state synthesis

The initial reagents used in this synthesis were Al_2O_3 (p.a.) and WO_3 (p.a.). Two separate experimental series were carried out. The reagents for the first series were homogenized in an agate mortar with subsequent pelletization and thermal treatment with different temperatures and duration. The second series included

* Corresponding author. Tel.: +359 2 979 2786; fax: +359 2 870 5024.
E-mail address: ikosseva@svr.igic.bas.bg (I. Koseva).

0925-8388/$ – see front matter © 2010 Elsevier B.V. All rights reserved.
doi:10.1016/j.jallcom.2010.06.100

Table 1
Thermal conditions and particle size of $Al_2(WO_4)_3$ solid state synthesis.

N	Temperature (°C)	Time of treatment (h)	Phase—XRD analysis	Medium size and morphology—TEM analysis	Remarks
1	750	72	WO_3		
2	810	48	WO_3		
3	870	24	$WO_3 + Al_2(WO_4)_3$		
4	930	16	$Al_2(WO_4)_3$ plus small amount of WO_3	66 nm, almost spherical	Pure $Al_2(WO_4)_3$ after second annealing
5	990	8	Pure $Al_2(WO_4)_3$		
6	1050	8	Pure $Al_2(WO_4)_3$	117 nm, slightly elongated	

also solid state synthesis but the initial reagents were homogenized in a ball mill with an agate container and agate balls. The weight ratio between ball and reagent amount was 10:1. The mechanical activation was realized at 200 rpm in the course of 6 h or in two cycles of 6 h each. The next step was pelleted and thermal treatment of the samples at different temperatures and duration.

2.2. Co-precipitation (CP)

$Al_2(WO_4)_3$ was prepared by mixing of aqueous solutions of $Al(NO_3)_3{\cdot}9H_2O$ (p.a.) and $Na_2WO_4{\cdot}2H_2O$ (p.a.) (0.1 M). The pH of the mixture thus obtained was 6.0. After stirring at room temperature for 10 h, the precipitate was collected, washed with distilled H_2O and dried at 80 °C for 5 h. This composition was further treated at 400, 630 and 830 °C for 5 h.

2.3. Sol–gel

The initial reagents were $Al(OH)_3$ (p.a.) and H_2WO_4 (p.a.). Citric acid was used as chelating agent and ethylene glycol—as estrification agent. $Al(OH)_3$ was dissolved in concentrated citric acid with a ratio between ions of 1:2. H_2WO_4 was dissolved in 25% NH_3 and added to the $Al(OH)_3$ solution with stirring. Then ethylene glycol was added in the ratio 1:1 with respect to the citric acid. The formed gel at 80 °C was dried in the course of 5 days at 90 °C. The so obtained product was treated first for 30 min at 300 °C until brown powder-like mass was obtained and then the temperature was raised to 600 °C at a rate of 150 °C/h. The light brown powder obtained after the last thermal regime was treated at different temperatures and for different duration until $Al_2(WO_4)_3$ was produced, as follows: 760 °C—72 h, 830 °C—12 h, 830 °C—36 h, 860 °C—12 h, 900 °C—2 h and 900 °C—6 h. The obtained product was white or light yellow powder according to the thermal conditions of the last treatment.

2.4. Characterization

Structural characterization was carried out by powder X-ray diffraction (XRD) using a Bruker D8 Advance powder diffractometer with Cu Kα radiation and SolX detector. XRD spectra were recorded at room temperature. Data were collected in the 2θ range from 10° to 80° with a step 0.04° and 1 s/step counting time. XRD spectra were identified using the Diffractplus EVA program.

The particle size and morphology were determined using a TEM JEOL 2100 at 200 kV. For this purpose specimens were prepared by grinding the samples in agate mortar and dispersing them in methanol by ultrasonic treatment for 6 min. A droplet of suspension was dispersed on holey carbon films on Cu grids. The particle size was determined using Lince v2.4—Linear Intercept program.

The thermal behaviour of some intermediate products was investigated by combined LABSYS^{TM} EVO DTA/TG device of the SETARAM Company, France. The samples were investigated at a heating rate of 10 °C/min in Ar flow at a flow rate of 20 ml/min.

3. Results and discussion

3.1. Solid state synthesis

The specific thermal conditions of synthesis, phase compositions and mean particle sizes of $Al_2(WO_4)_3$ are presented in Table 1.

As seen in the table, to produce a pure product, $Al_2(WO_4)_3$, a minimal time for thermal treatment at a given temperature is required and naturally, this time is longer for the lower temperatures. The minimum temperature for obtaining pure $Al_2(WO_4)_3$ is 930 °C, for duration of 32 h.

Fig. 1 shows the X-ray diffraction patterns of the products after solid state synthesis at 810, 930 and 1050 °C without preliminary

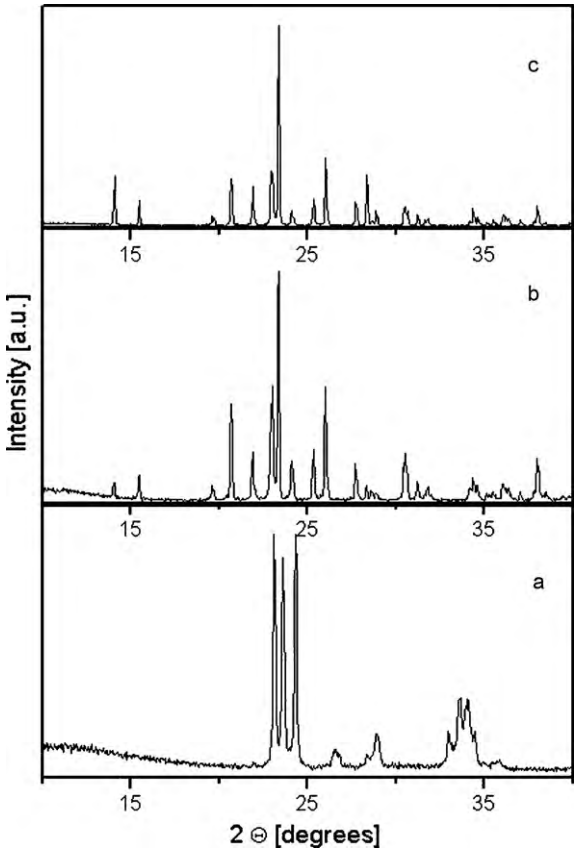

Fig. 1. X-ray diffraction patterns of the products obtained by solid state synthesis at different temperatures and times: (a) 810 °C for 48 h; (b) 930 °C for 16 h and (c) 1050 °C for 8 h.

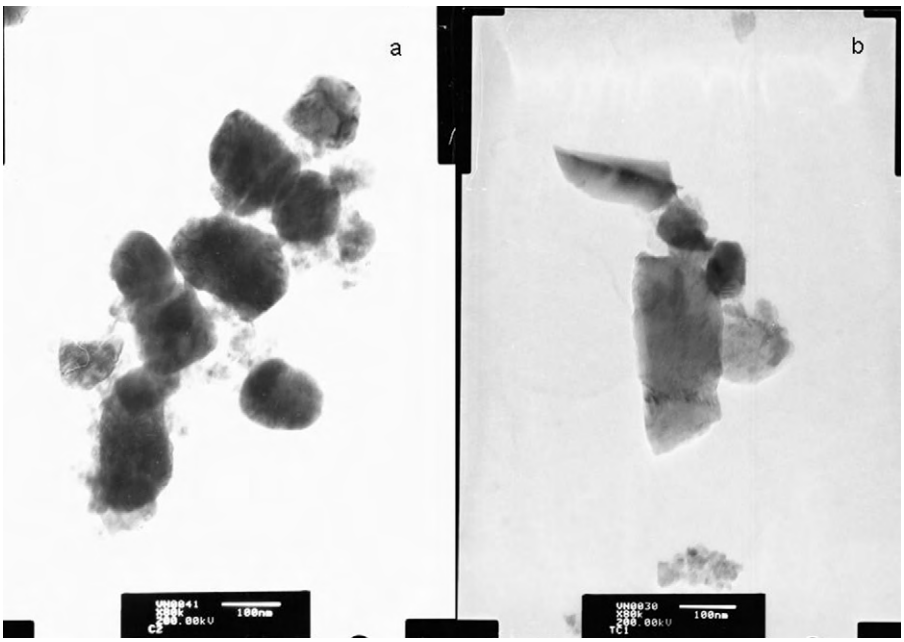

Fig. 2. TEM images of $Al_2(WO_4)_3$ obtained by solid state synthesis: (a) 930 °C for 16 h and (b) 1050 °C for 8 h.

mechanical activation. The X-ray patterns for the two lower temperatures show the presence of unreacted WO_3.

The results of the solid state syntheses after preliminary mechanical activation are qualitatively the same. The difference consists in the fact that the minimum temperature for obtaining pure $Al_2(WO_4)_3$ is with about 100 °C lower.

Fig. 2 shows the TEM images of products after solid state synthesis at 930 °C (a) and 1050 °C (b). The mean particle size dimension of $Al_2(WO_4)_3$ is 66 and 117 nm after treatment at 930 °C and at 1050 °C respectively. The morphology changes from near spherical to elongated. No visible difference is observed for the particles treated at minimum temperatures with and without preliminary mechanical activation. There is also no difference in the growth rate of the particles with increasing the temperature of synthesis.

Fig. 3 shows the size distribution after treatment at 930 °C (a) and 1050 °C (b). As can be seen, the particles are distributed between 20 and 120 nm at the lower temperature and rise up to 60–150 nm at 1050 °C.

3.2. Co-precipitation

Fig. 4 presents the X-ray diffraction patterns of the products after co-precipitation and subsequent thermal treatment in the course of 5 h at 80, 400, 630 and 830 °C. As seen in the figure, the products at 80 and 400 °C are amorphous, at 630 °C well crystallized $Al_2(WO_4)_3$ is observed, and at 830 °C the product is well crystallized without an amorphous phase.

The DTA analysis (Fig. 5) shows that the amorphous product obtained at 80 °C contains about 10 wt% of weight loss, which is released with a maximum at 200 °C. The crystallization of $Al_2(WO_4)_3$ is related with an sharp exothermal effect with a maximum at about 600 °C.

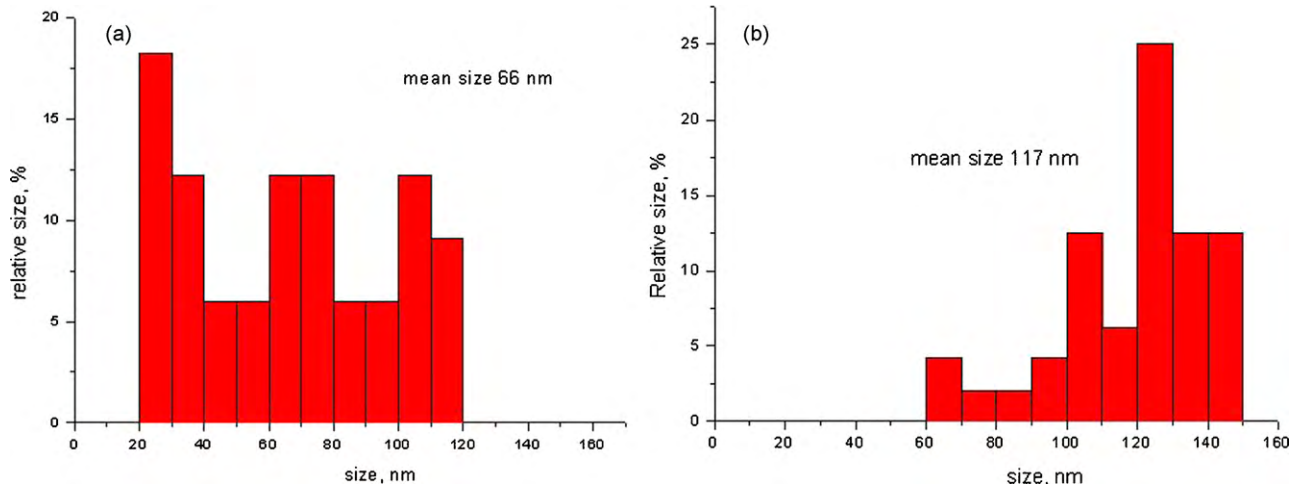

Fig. 3. Size distribution after solid state reaction at 930 °C (a) and 1050 °C (b).

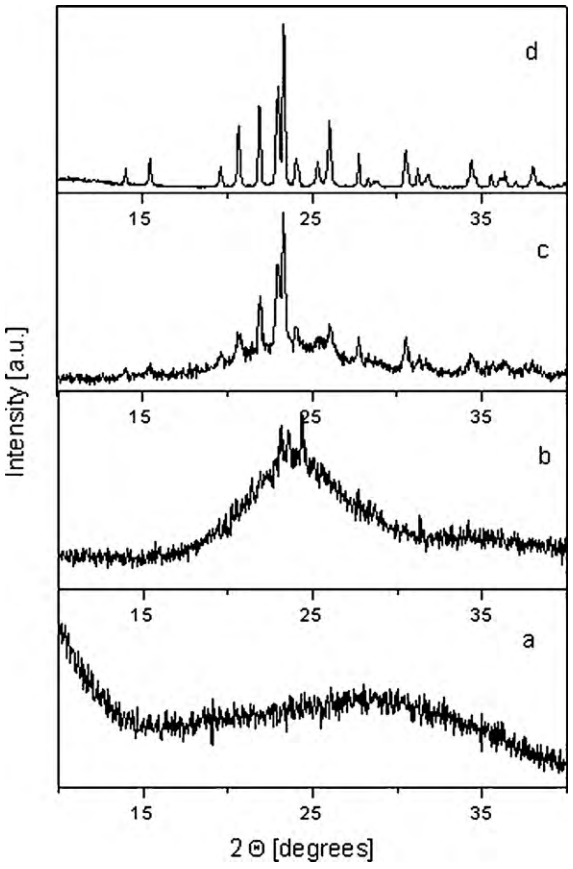

Fig. 4. X-ray diffraction patterns of the products obtained by co-precipitation after 5 h of final thermal treatment at different temperatures (a) 80 °C, (b) 400 °C, (c) 630 °C and (d) 830 °C.

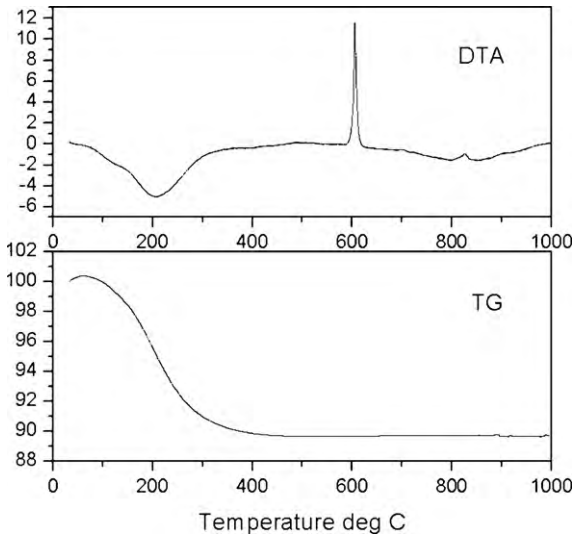

Fig. 5. DTG-TG of a sample from co-precipitation after 5 h of thermal treatment at 80 °C.

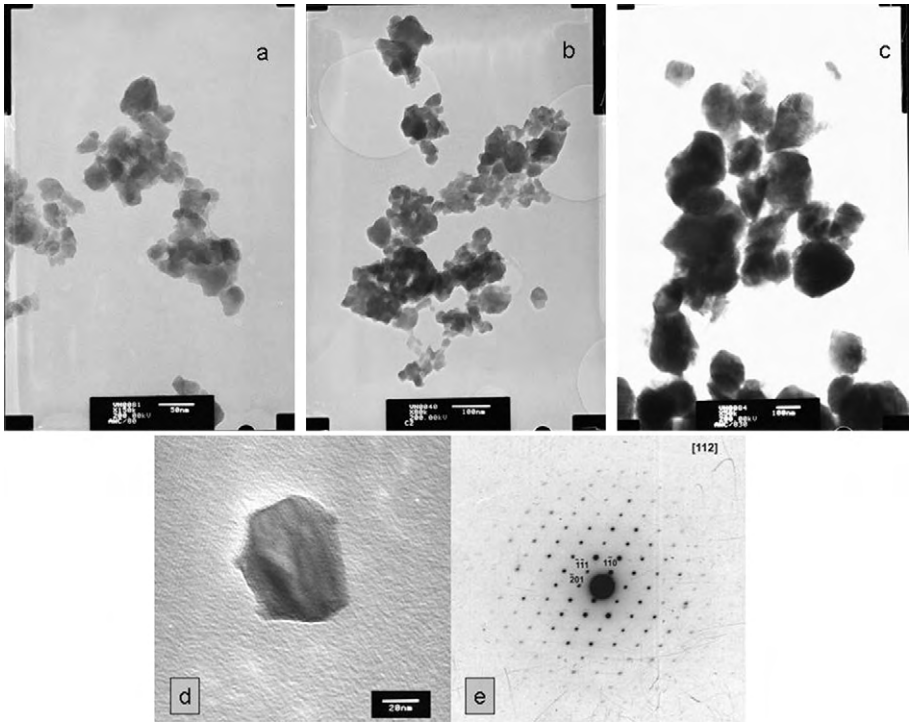

Fig. 6. TEM images of $Al_2(WO_4)_3$ obtained by co-precipitation and thermal treatment at different temperatures: (a) 80 °C, (b) 630 °C and (c) 830 °C. Bright field micrograph of $Al_2(WO_4)_3$ particle after treatment at 630 °C (d) and SEAD of the particle along [1 1 2] orientation (e).

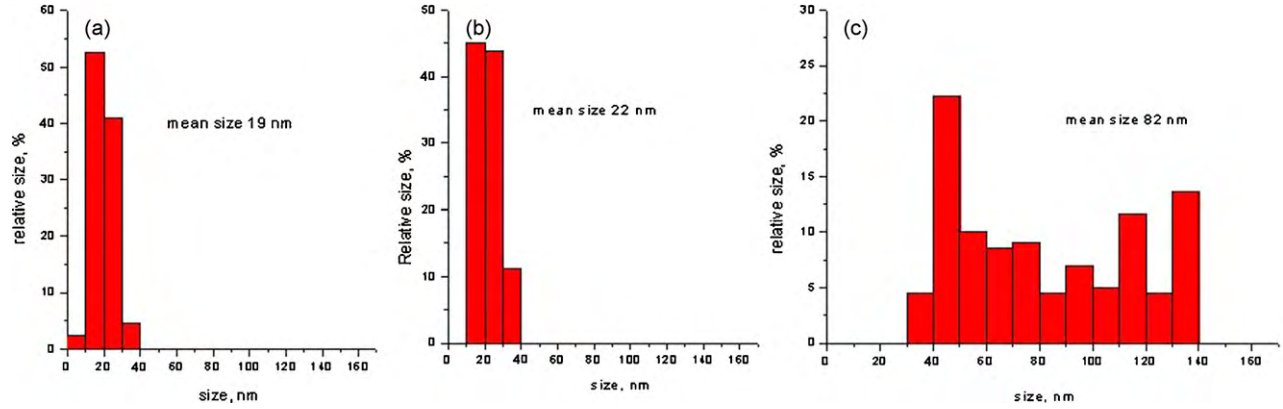

Fig. 7. Size distribution of the particles obtained by co-precipitation method after 5 h treatment at 80 °C (a), 630 °C (b) and 830 °C.

The TEM images of the products, treated at 80, 630 and 830 °C, are shown in Fig. 6 (a–c). The spherical particles at 80 °C with mean size of 19 nm almost preserve their sizes and shape at 630 °C (22 nm). A quick particle growth is observed at 830 °C to 82 nm, with a slightly trend for elongation in one direction.

The mean crystallite sizes were estimated using the integral breadth of the picks profile according to the Sherrer equation. The whole powder pattern Pawley fit method was employed using Topas 3 program (Bruker AXS, TOPAS V3; General profile and structure analysis software for powder diffraction data, User's manual, Bruker AXS, Karlsruhe, Germany 2005). For the particles dimensions were received 35.6 and 88.8 nm for 630 and 830 °C respectively.

Fig. 7 shows the size distribution of the particles. The important result is, that the particles are distributed in a narrow region from 10 to 40 nm for 80 and 630 °C. This means that particle dimensions remains intact after the crystallization of amorphous $Al_2(WO_4)_3$ at 630 °C. A significant particle growth takes place when $Al_2(WO_4)_3$ is heated at 830 °C: the particle sizes are distribution from 30 to 140 nm. It is important that the particle growth slightly affects the isometric particle shape, irrespective of the anisotropic structure of $Al_2(WO_4)_3$.

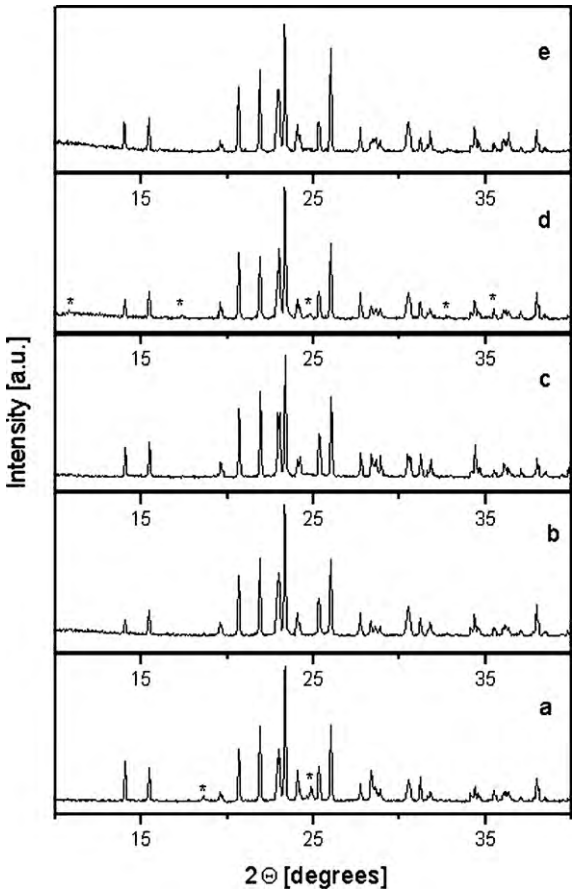

Fig. 8. X-ray diffraction patterns of the samples obtained by sol–gel method treated at different temperature and different heating time: (a) at 760 °C for 72 h, (b) at 830 °C for 36 h, (c) at 860 °C for 12 h, (d) at 900 °C for 2 h and (e) at 900 °C for 6 h.

3.3. Sol–gel (modified method of Pechini)

The X-ray patterns of $Al_2(WO_4)_3$ obtained from the sol–gel method and heated at 760 °C (for 72 h), 830 °C (for 36 h), 860 °C (for 12 h) and 900 °C (for 2 and 6 h) are shown in Fig. 8.

As one can see, a pure $Al_2(WO_4)_3$ phase is obtained at temperatures above 830 °C. At lower temperatures and shorter heating times another phase is also detected in the product and its quantity decreases with increasing of the temperature. The composition of this phase has not been established at this stage of research. It seems that this phase is formed even at lower temperatures and it is related with the presence of carbon in the polymeric resin. The ground for such a hypothesis is the fact that the longer treatment of the products at low temperatures hampers additionally the subsequent purification (removal) of this phase. Furthermore, the thermal treatment of the polymeric resin in an oxygen flow instead in an air leads to the formation of a pure $Al_2(WO_4)_3$ product as early as at 630 °C.

The TEM images of the end $Al_2(WO_4)_3$ products obtained by means of the sol–gel method and finally treated at 630 °C in air and at 830 °C are shown in Fig. 9. The impressive difference in the size and shape of the particles of pure $Al_2(WO_4)_3$ is obvious. The treatment at 630 °C results in slightly elongated shapes with medium size of 33 nm, while the particles treated at 830 °C are with elongated form and medium size of 103 nm. According to the Sherrer equation for the particles dimensions were received 119.4 and 248.0 nm for 630 and 830 °C respectively.

Fig. 10 shows that the particles are distributed in region between 10 and 60 nm for 630 °C and grow up to 60–150 nm at 830 °C.

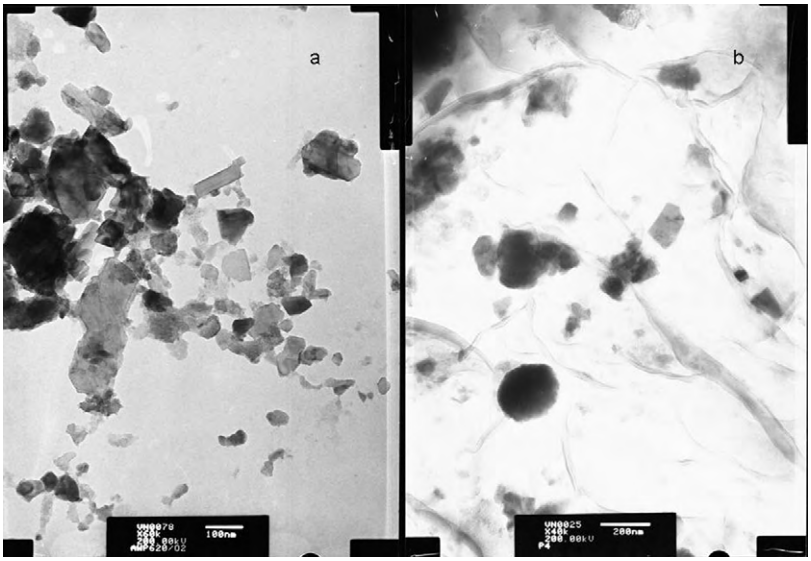

Fig. 9. TEM images of $Al_2(WO_4)_3$ obtained by the modified method of Pechini after thermal treatment at (a) 630 °C for 36 h; (b) 830 °C for 5 h.

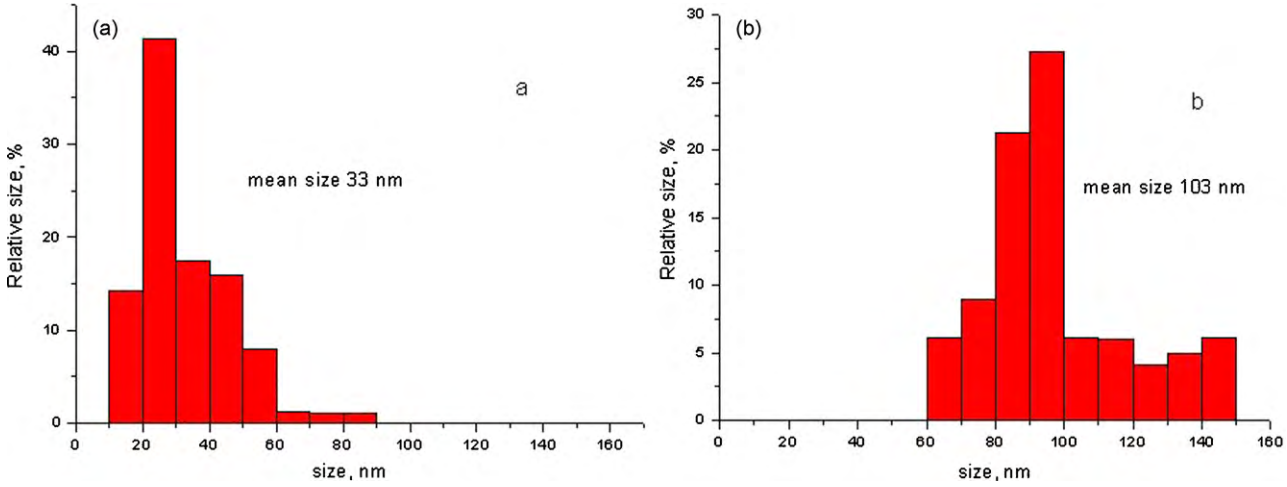

Fig. 10. Size distribution of the particles obtained by sol–gel method after treatment at (a) 630 °C for 36 h and (b) 830 °C for 5 h.

4. Conclusions

The investigations carried out show the possibility of producing pure $Al_2(WO_4)_3$ according to the three methods—solid state synthesis, co-precipitation and sol–gel. In spite of this the final results about particle size, morphology, size distribution and the reactivity (particle growth during the thermal treatment) are very different. Co-precipitation method gives lowest in size, uniform particles, distributed in very narrow size region. In addition these particles grow quickly, expanding more than four times during the thermal treatment. In the opposite, the solid state process gives bigger particles, distributed in a wide region, growing very slowly. Sol–gel method is in the middle position from this point of view.

From the viewpoint of producing optically transparent ceramics, the most suitable product for further sintering seems to be the $Al_2(WO_4)_3$ produced by co-precipitation. The small size of the particles, their shape and trend to faster growth with temperature rise, presume the possibility of strong crystallization and densification of the ceramics until transparency is reached. The conditions for producing such ceramics will be the object of further investigations.

Acknowledgements

The authors are indebted to the National Science Fund of Bulgaria (Contract no. DO02-216/2008) for financial support. The authors acknowledge also the National Centre for New Materials UNION (Contract No. DO-02-82/2008).

References

[1] K. Nassau, H.J. Levinstein, G.M. Loiacono, J. Phys. Chem. Solids 26 (1965) 1805–1816.
[2] N. Imanaka, Y. Kobayashi, S. Tamura, G. Adachi, Electrochem. Solid State Lett. 1 (1998) 271–273.
[3] N. Imanaka, M. Kamikawa, S. Tamura, G. Adachi, Solid State Ionics 133 (2000) 279–285.
[4] G. Adachi, N. Imanaka, S. Tamura, J. Alloys Compd. 323–324 (2001) 534–539.
[5] J.S.O. Evans, T.A. Mary, A.W. Sleight, J. Solid State Chem. 133 (1997) 580–583.
[6] T.A. Mary, A.W. Sleight, J. Mater. Res. 14 (1999) 912–915.
[7] T. Sugimoto, Y. Aoki, E. Niwa, T. Hashimoto, Y. Morito, J. Ceram. Soc. Jpn. 115 (2007) 176–181.
[8] K. Petermann, P. Mitzscherlich, IEEE J. Quant. Electron. 23 (1987) 1122–1126.
[9] Y. Kobayashi, N. Imanaka, G. Adachi, J. Cryst. Growth 143 (1994) 362–364.
[10] N. Imanaka, M. Hiraiwa, S. Tamura, G. Adachi, H. Dabkowska, A. Dabkowski, J. Cryst. Growth 200 (1999) 169–171.

[11] A. Dabkowski, H.A. Dabkowska, J.E. Greedan, G. Adachi, Y. Kobayashi, S. Tamura, M. Hirakawa, N. Imanaka, J. Cryst. Growth 197 (1999) 879–882.
[12] N. Imanaka, M. Hiraiwa, G. Adachi, H. Dabkowska, A. Dabkowski, J. Cryst. Growth 220 (2000) 176–179.
[13] D. Ivanova, V. Nikolov, P. Peshev, J. Cryst. Growth 308 (2007) 84–88.
[14] D. Ivanova, V. Nikolov, P. Peshev, J. Alloys Compd. 430 (2007) 356–360.
[15] D. Ivanova, V. Nikolov, R. Todorov, J. Cryst. Growth 311 (2009) 3428–3434.
[16] C. Li, H. Zuo, M. Zhang, J. Han, S. Meng, Trans. Nonferrous Met. Soc. China 17 (2007) 148–153.
[17] H. Huang, H. Gong, D. Tang, O. Tan, Opt. Mater. 31 (2009) 716–719.
[18] H. Yagi, T. Yanagitani, K. Takaichi, K. Ueda, A. Kaminskii, Opt. Mater. 29 (2007) 1258–1262.
[19] X. Li, Q. Li, J. Wang, S. Yang, H. Liu, Opt. Mater. 29 (2007) 528–531.
[20] S.N. Bagayev, V.V. Osipov, M.G. Ivanov, V.I. Solomonov, V.V. Platonov, A.N. Orlov, A.V. Rasuleva, S.M. Vatnik, Opt. Mater. 31 (2009) 740–743.
[21] J. Li, Y. Wu, Y. Pan, W. Liu, L. Huang, J. Guo, Opt. Mater. 31 (2008) 6–17.
[22] J. Li, Y. Wu, Y. Pan, H. Kou, Y. Shi, J. Guo, Ceram. Int. 34 (2008) 1675–1679.
[23] D. Zhou, Y. Shi, P. Yun, J.J. Xie, J. Alloys Compd. 479 (2009) 870–874.
[24] J. Zhang, L. An, M. Liu, S. Shimai, S. Wang, J. Eur. Ceram. Soc. 29 (2009) 305–309.
[25] A.C. Bravo, L. Longuet, D. Autissier, J.F. Baumard, P. Vissie, J.L. Longuet, Opt. Mater. 31 (2009) 734–739.